Radiography 25 (2019) 72–76

Contents lists available at ScienceDirect

Radiography

journal homepage: www.elsevier.com/locate/radi

Simultaneous measurement of patient dose and distribution of indoor scattered radiation during digital breast tomosynthesis

T. Nakamura [a, e, *], S. Suzuki [a], Y. Takei [b], I. Kobayashi [c], N. Pongnapang [d], K. Kato [e]

[a] Department of Radiology, Daido Hospital, Japan
[b] Department of Radiological Technology, Kawasaki University of Medical Welfare, Kawasaki, Japan
[c] Nagase Landauer, Inc., Japan
[d] Department of Radiological Technology, Faculty of Medical Technology, Mahidol University, Siriraj Hospital, Thailand
[e] Showa University Graduate School of Health Sciences, Japan

ARTICLE INFO

Article history:
Received 12 June 2018
Received in revised form
22 October 2018
Accepted 23 October 2018
Available online 15 November 2018

Keywords:
Digital breast tomosynthesis
Scatter dose
Average glandular dose (AGD)
Entrance surface dose
Radiation safety
Jungle gym method

ABSTRACT

Introduction: Breast cancer incidence increases from the age of 30 years. As this age range coincides with that in which women usually pursue pregnancy, undergoing medical examinations for conditions such as breast cancer is a concern, especially when pregnancy is uncertain during the first eight weeks. Moreover, in this age range, breast often exhibits a high density, thus compromising diagnosis. For such density, digital breast tomosynthesis (DBT) provides a more accurate diagnosis than 2D mammography given its higher sensitivity and specificity. However, radiation exposure increases during DBT, and it should be determined.
Methods: We determined the entrance surface dose, scattered radiation dose, and average glandular dose (AGD), which can be mutually compared following an international protocol. Using our proposed method, the distribution of scattered radiation can be easily and quickly obtained with a minor load to the equipment. Then, we can determine the indoor scattered radiation and surface dose on patients during DBT.
Results: We obtained a maximum AGD of 2.32 mGy. The scattered radiation was distributed over both sides with maximum of approximately 40 μGy, whereas the maximum dose around the eye was approximately 10 μGy.
Conclusion: By measuring doses using the proposed method, a correct dose information can be provided for patients to mitigate their concerns about radiation exposure. Although the obtained doses were low, their proper management is still required. Overall, the results from this study can help to enhance dose management for patients and safety management regarding indoor radiation.

Introduction

Over the last decades, delayed pregnancy has been constantly increasing in Japan given changes in society's priorities. According to a survey published by the Ministry of Health, Labour and Welfare of Japan from 2014, the average age of women giving birth for the first time has increased to 30.6 years old, with an increasing trend in this age. This situation also occurs in countries such as Greece, Australia, and South Korea.[1] As the risk of delivery increases with age, women actively attempting to get pregnant by engaging in fertility treatments[2] outnumber those waiting for natural pregnancy.

On the other hand, breast cancer incidence in Japan peaks at ages around 50 years and slightly reduces afterwards, but in Europe and America, the incidence continues to rise after the age of 50.[3] Therefore, it is usual that many women undergoing mammography, which is recommended for women who reach 40 years old onwards, also are actively seeking pregnancy. Likewise, many women in their thirties undergo screening mammography. However, the overlapping range of ages for breast cancer examination and pursuit of pregnancy makes women concern about undergoing examination when they are unaware of pregnancy, usually between the first and eighth week. Moreover, the breast during this age

* Corresponding author. Department of Radiology, Daido Hospital, 9 Hakusui-cho, Minami-ku, Nagoya, Aichi 457-8511, Japan.
E-mail address: tokikonakamura1095@yahoo.co.jp (T. Nakamura).

https://doi.org/10.1016/j.radi.2018.10.006
1078-8174/

range tends to exhibit high density, thus compromising the discovery of abnormalities such as tumors and cancer. Although ultrasound is recommended for breast cancer examination among women in their thirties, including those who are pregnant,[4] differences in the diagnostic capabilities arise given conspicuous technological differences among scanners. In contrast, mammography screening has been scientifically proven to decrease mortality by its accuracy, but this has not been verified on other tests such as ultrasound. Likewise, adding tomosynthesis to mammography increases the diagnostic ability, and hence the use of this technique is expected to increase in the coming years.

In fact, digital breast tomosynthesis (DBT) has become popular for assessing breast cancer. DBT is a 3D radiographic imaging technology that irradiates a pulse-like X-ray on the compressed breast, in a manner similar to conventional 2D digital mammography, while moving the X-ray tube to acquire images at multiple angles. Then, the individual images are reconstructed as a sequence of thin high-resolution tomograms.[5,6] DBT-based mammography outperforms 2D mammography in the diagnosis capability given the improved sensitivity and specificity.[7] However, DBT implies a higher radiation exposure than 2D mammography.[8] Consequently, the risk for the radiation dose increases during DBT, implying higher risks for every patient, but with especial caution required for women attempting pregnancy. The effects of such radiation exposure among patients should be carefully evaluated. Likewise, properly understanding the exposure dose during DBT by health professionals would improve the assessment from the examination and provide information on the risks and benefits for the emotional care of patients.

To correctly evaluate radiation during DBT, the average glandular dose (AGD), entrance surface dose on patient, and scatter dose should be measured. Although several studies evaluate the AGD during DBT, the simultaneous evaluation of the patient dose and her surrounding space has not been conducted, and the appropriate measurement method has yet to be identified.[9] Moreover, tomosynthesis consists of an examination with moving and irradiating equipment, and given that its distribution differs from that of conventional 2D mammography, we measured the DBT scattered radiation in this study. We aimed to evaluate the incident dose, external exposure dose, and scattered radiation dose with respect to the examinee in the same dimension. In particular, the distribution of scattered radiation should be assessed by the examiner in some circumstances, e.g., at the position of a caregiver when the examinee requires assistance. In this study, we aimed to determine the AGD during DBT and evaluate the entrance surface dose and scatter dose using simultaneous measurements, thus proposing a new radiation evaluation method for DBT.

Methods

Scatter dose in the examination room

We used the AMULET Innovality DBT system (Fujifilm Holdings Co., Tokyo, Japan) for imaging, the Accu-Gold + system (Radcal Co., Monrovia, CA, USA) for X-ray measurement analysis, and the AGMS-DM + multi-sensor (Radcal Co., Monrovia, CA, USA) along with a 40 mm thick Polymethylmethacrylate (PMMA) phantom (Fujifilm Holdings Co., Tokyo, Japan) to perform semiconductor detection. We set the tube voltage to 31 kV, the current–exposure time product to 56 mAs, and the target/filter to W/A1. In addition, we used the nanoDot optically stimulated luminescence dosimeter (Landauer, Inc., Glenwood, IL, USA) to measure the scatter dose. The detector was compatible with a Japanese standard, and every element in the nanoDot dosimeter was calibrated. Moreover, 50-cm long radiolucent paper cylinders resistant to X-ray absorption were used to construct a 200 × 200 × 150 cm gridwork resembling a jungle gym. Such paper cylinders exhibit low attenuation and scattering for low interference with the measurement results. We attached 90 optically stimulated luminescence dosimeters on the vertices of the gridwork to measure scatter radiation dose at multiple points. Then, to visualize the distribution of scatter dose, we generated a color map. Measurements were taken from two projections, namely, craniocaudal (CC) and right mediolateral oblique (R-MLO) views. The phantom was used as scatterer and matched with the chest wall terminal of a breast holding plate to align the compression plate and the left, right, and center of the holding plate such that it was adjacent to the upper side of the phantom. DBT was conducted 20 times to measure scatter dose from the measurement points shown in Fig. 1.

Entrance surface dose

To simultaneously measure the entrance surface dose and scatter dose, we attached the nanoDot optically stimulated luminescence dosimeters on positions corresponding to eyes (right 1, left 2), thyroid (right 3, left 4), abdmen (5), and reproductive gland (right 6, left 7) of the anthropomorphic RAN110 phantom (The Phantom Laboratory, Inc., Salem, NY, USA), as shown in Fig. 2. The imaging setup and parameters were the same as those for the scatter dose measurements detailed in the previous section.

Average glandular dose

We determined the AGD from both 2D and DBT mammography by following the European Reference Protocol for the Quality Control of the Physical and Technical Aspects of Digital Breast Tomosynthesis Systems, version 1.01 published in June 2016.[10] The effective center of the dosimeter was placed at 6 cm from the chest wall side and 4 cm height. For measuring the AGD, we used the semiconductor detection. In addition, the compression plate was aligned to be adjacent to the detector. The same tube voltage and current–exposure time product mentioned above were used, but the target/filter was set to W/Rh. The AGD was calculated considering the kerma and half-value layer. The AGD during 2D mammography was calculated as

$$D = K \times g \times c \times s \quad (1)$$

where D is the AGD for 2D mammography in mGy, K is the air kerma at the entrance surface, g is the coefficient equivalent to 50% of glandular content rate, c is the coefficient that corrects different glandular content from 50% glandular content rate, and s is the coefficient for the combination of target and filter.

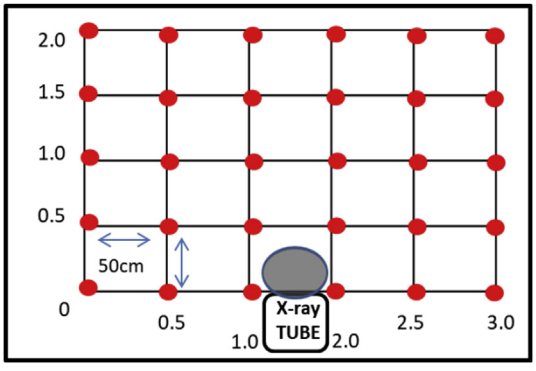

Figure 1. Scattered radiation measurement points. (The grid-axis units are meters.)

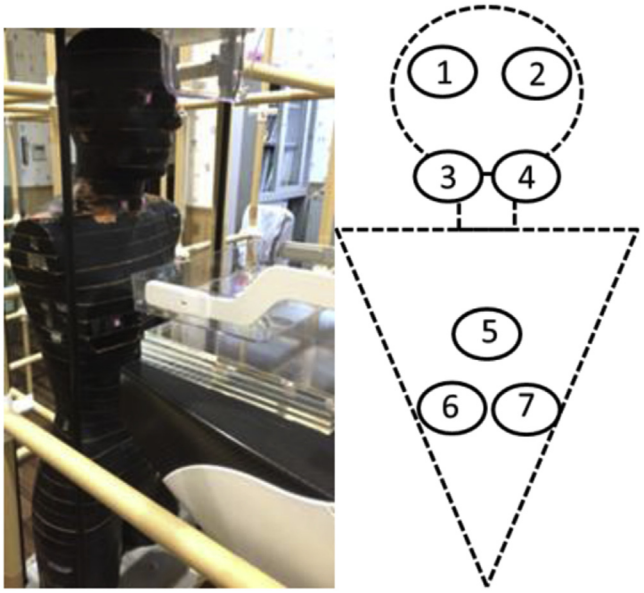

Figure 2. Measurement positions at the eyes, thyroid, and gonad of the RAN110 phantom.

We applied a series of pulsed irradiation for DBT with the X-ray tube fixed along the CC direction (oscillation angle $\theta = 0°$) and rotated (oscillation angle $\theta = 20°$). Like for 2D mammography, the AGD for DBT mammography was calculated from the obtained kerma and half-value layer as

$$D_T = K_T \times g \times c \times s \times T(\theta) \quad (2)$$

where D_T is the AGD for DBT in mGy, K_T is the air kerma at the entrance surface measured from irradiation for the DBT images at oscillation angle $\theta = 0°$, coefficients g, s, and c are the same as those for 2D mammography in equation (1),[11,12] and coefficient T corrects variations caused by oscillation angle θ and equipment radiation, as listed in values determined from the Protocol for the Quality Control of the Physical and Technical Aspects of Digital Breast Tomosynthesis Systems, version 1.01.[10]

Results

Scatter dose in the examination room

Fig. 3 shows the distribution of scatter dose in the examination room. At each measurement position, the dose was symmetrically distributed at the left and right sides for the CC view, whereas the distribution was higher on the right side for the R-MLO view. In addition, the scatter dose decreased at the posterior region of the phantom for both the CC and R-MLO values. Specifically, the highest value was 44 μGy at 50 cm on the left and right sides from the center of the beam at a height of 150 cm above the floor for the CC view. Similarly, the maximum value of 40 μGy was observed at 50 cm on the right side of the phantom from the center of the beam at a height of 150 cm above the floor for the R-MLO view. The dose was below 1 μGy for both the CC and R-MLO views at a distance beyond 150 cm from the beam.

Entrance surface dose

Table 1 lists the entrance surface dose for each organ. The difference between the left and right sides for the entrance surface dose at each organ position was very small in the CC view, but the right side showed higher doses in most organs, except for the gonads whose doses were the same, in the R-MLO view. The dose at the eyes position was 10.3 μGy for the CC view and 5.6 μGy on the right side for the R-MLO view, whereas that at the gonad position was even lower with 1.0 μGy for the CC view and 0.4 μGy for the R-MLO view.

Average glandular dose

The entrance air kerma in the CC view for 2D mammography was 3.404 mGy and by using coefficients $g = 0.309$, $s = 1.04$, and $c = 1.035$, we obtained an AGD of 1.14 mGy. The entrance air kerma in the CC view with fixed X-ray tube (i.e., $T(\theta) = 0°$) for DBT mammography was 6.921 mGy and by using coefficients $g = 0.306$, $s = 1.082$, $c = 1.04$, and $T = 0.972$ ($\pm 20°$), we obtained an AGD of 2.32 mGy. Likewise, considering the rotating X-ray tube (i.e., $T(\theta) = 20°$) for DBT mammography, an entrance air kerma in the CC view of 6.732 mGy, and coefficients $g = 0.299$, $s = 1.082$, $c = 1.04$, and $T = 1.00$, we obtained an AGD of 2.26 mGy (see Table 2).

Discussion

We found a slight difference of 0.06 mGy with ±2% error between the AGD without rotation (2.32 mGy) and with oscillation angle of 20° (2.26 mGy). In addition, the ratio of entrance air kerma between the fixed and rotating X-ray tube was 0.973, which was a value close to that of coefficient T. Although the directionality and projection angle of the dosimeter should be considered, the results suggest that this ratio may be used as the T value. According to Dance,[13] the AGD at rotating angle $T(0°)$ corresponds to the AGD when rotating at angle θ over the AGD for no rotation ($\theta = 0°$), which shows that T is the average value of coefficient $T(\theta)$ for correcting the oscillation angle of each X-ray tube for a given X-ray output. Moreover, the AGD at angle θ and AGD at angle 0° are equivalent to $g \times s \times c$ when irradiating onto the same subject, where the only varying factor is the entrance air kerma. Therefore, the ratio of entrance air kerma between rotating and fixed X-ray tube can be used as the T value.[14] However, further considerations are required as the entrance air kerma may not be measured correctly depending on the rotating angle of the imaging device. In this study, we calculated the AGD using a phantom, but the calculation of the radiation exposure for a real patient is more complex as the correct c value and equivalent thickness of the compressed breast must be determined.

The entrance surface dose of the phantom and scatter dose distribution in the examination room varied depending on the imaging direction. This distribution enabled the evaluation, for example, of the dose received at the position of a caregiver when a patient requires assistance (e.g., wheelchair dependent). In fact, we considered that the distribution can be evaluated by the incident surface dose because the energy and dose are low, as shown from the measurements. Likewise, as the doses reported in this study are very low, only stochastic risks should be considered. When calculating the AGD under the abovementioned European Reference Protocol,[10] no changes in the imaging direction were observed as measurements were taken at 0°, where the X-ray tube is vertical against the flat panel detector regardless of the imaging direction and beam angle. However, the entrance surface dose and scatter dose in the examination room was affected by the radiographic direction. Specifically, the entrance surface dose was symmetrical between left and right for each organ position around the CC view, because the swing is symmetrical to the left and right in this view with 0° as baseline. However, the R-MLO view involves an exposure leaning to the right as the X-ray tube is tilted in that direction, and

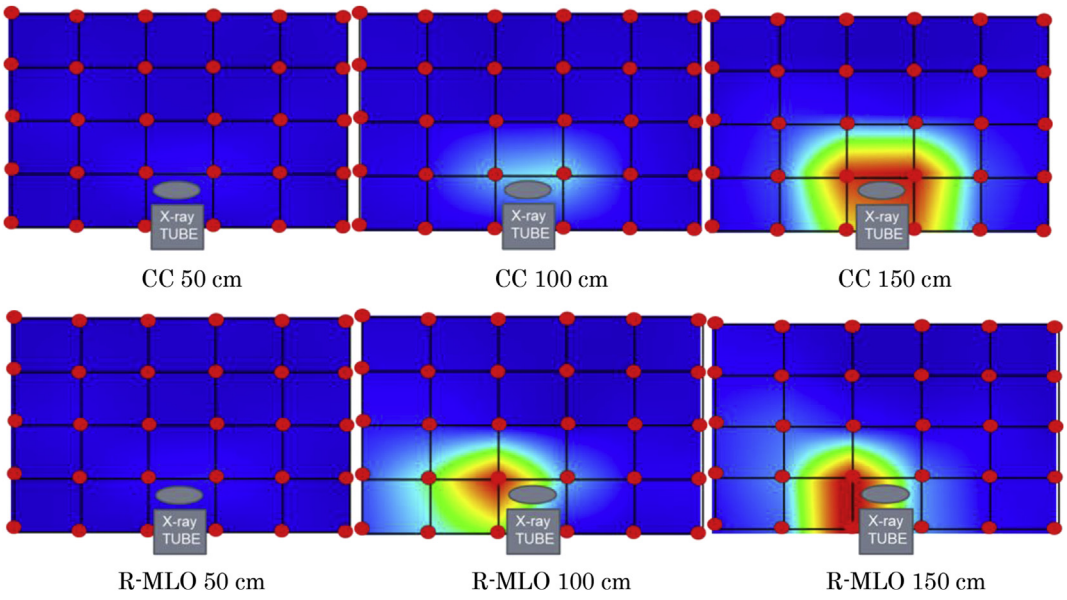

Figure 3. Scattered radiation distribution in the examination room.

Table 1
Surface dose at each organ position.

Organ	Surface dose (μGy)	
	CC	R-MLO
1. Left eye	9.1	3.6
2. Right eye	10.3	5.6
3. Left lobe of thyroid	8.3	5.1
4. Right lobe of thyroid	7.7	6.3
5. Abdomen	2.1	1.3
6. Left gonad	1.0	0.4
7. Right gonad	1.0	0.4

hence it is expected that the right side, which is closer to the X-ray tube, receives a higher radiation. We were able to correctly identify the distribution of scatter dose in the examination room by using the proposed measurement method. The scatter radiation dose was 1, 27, and 44 μGy at heights of 50, 100, and 150 cm, respectively, whereas the entrance surface dose at the eyes position in the phantom was 5.1 μGy. These values show that the radiation impact on the eyes and surroundings of the patient is also negligible.

The entrance surface dose is the air absorbed dose that includes the posterior scatter on the skin surface. This dose is used in the radiography field following the diagnostic reference levels of Japan, last updated in 2015, where the AGD is used to evaluate radiation exposure in mammography and has a value of 2.4 mGy, which is very close to the measured AGD value during DBT mammography in this study. For a patient with an average breast that contains 50% fat, 50% mammary gland, and is 40 mm thick undergoing examination, the entrance surface dose will be equal to that obtained from the phantom in this study. Although the entrance surface dose of the breast receives a low energy level, it is still much larger than the dose in other parts of the general radiographic area, namely, radiography, angiography, fluoroscopy, mammography, and the diagnostic reference levels. Hence, the proper exposure management for patients is critical during DBT mammography.[15,16]

The dosimeters facing the X-ray tube are maintained in fixed positions on the gridwork vertices. Therefore, the proposed measurement method applied for scattered measurements allows to fix dosimeter elements to any required position, and hence it provides a high reproducibility. In addition, the researcher taking measurements does not get exposed to radiation, unlike some conventional methods in which the experimenter is exposed to radiation and must wear a protective gear to determine the indoor dose distribution. Moreover, the proposed method allows to perform radiation safety management for the patient. The indoor scattered radiation measurement using the proposed method is easy to setup and fast to retrieve results, thus reducing the load to the equipment. Therefore, radiation safety management is possible in addition to dose management for patients, and the proposed method can be applied for measurements at any facility. Furthermore, the proposed method allows to simultaneously determine the AGD, dose outside the beam, and indoor scattered dose distribution for DBT mammography, and thoroughly analyze this information in a timely manner. In this study, we tested a relatively low dose level that can be affected by background noise, because we aimed to demonstrate the effectiveness and applicability of the measurement setup. In future studies, we will increase the dose range and number of measurements using the proposed setup.

Table 2
AGD for 2D and DBT-based mammography.

Condition			Measured value		Calculated value				
T/F	Tube voltage (kV)	Current–exposure time product (mAs)	HVL (mmAl)	Dose (mGy)	s-Factor	g-Factor	c-Factor	T-Factor	AGD (mGy)
2D:W/Rh	31	50	0.54	3.404	1.042	0.309	1.04	–	1.14
DBT 0°: W/Al			0.54	6.921	1.082	0.306	1.04	0.972	2.32
DBT 20°: W/Al			0.53	6.732	1.082	0.299	1.04	1.00	2.26

Conclusion

This study revealed the characteristics and dose of DBT through measurements. Its usefulness became clear as the dose outside the beam and the distribution of scatter dose in the examination room can be simultaneously measured and determined, thus establishing a new measurement approach. The results from applying the proposed method can serve as basis for educating health professionals involved in radiographic examination about radiation safety. By correctly communicating the obtained data to patients, the results of this study can help to mitigate their concerns about radiation exposure.

Conflict of interest statement

All authors declare that there are no conflicts of interest.

Acknowledgments

We would like to express our gratitude to director Hirofumi Anno and technical director Satoru Kamiya of the Department of Radiation at the Daido Hospital, Japan, and to the many staff members for their support and guidance throughout this study.

This research did not receive any specific grant from funding agencies in the public, commercial, or not-for-profit sectors.

References

1. The Central Intelligence Agency. *The world factbook 2013*. https://www.cia.gov/library/publications/download/download-2013/ [accessed 09.08.18].
2. Saito H, Shirakaw M. *Pregnant bible life planning of a woman living in the era of late marriage and declining birthrate*. Kodansha Ltd+αshinsyo; 2012 [in Japanese].
3. World Health Organization. *International agency for research on cancer*. https://gco.iarc.fr/today/home [accessed 22.07.18].
4. Ohuchi N, Suzuki A, Sobue T, Kawai M, Yamamoto S, Zheng YF, et al. Sensitivity and specificity of mammography and adjunctive ultrasonography to screen for breast cancer in the Japan Strategic Anti-cancer Randomized Trial (J-START): a randomised controlled trial. *Lancet* 2015;**387**:341–8. https://doi.org/10.1016/S0140-6736(15)00774-6.
5. Niklason LT, Christian BT, Niklason LE, Kopans DB, Castleberry DE, Opsahl-Ong BH, et al. Digital tomosynthesis in breast imaging. *Radiology* 1997;**205**:2399–406. https://doi.org/10.1148/radiology.205.2.9356620.
6. Dobbins III JT, Godfrey DJ. Digital x-ray tomosynthesis: current state of the art and clinical potential. *Phys Med Biol* 2003;**48**:65–106. https://doi.org/10.1088/0031-9155/48/19/R01.
7. Vedantham S, Karellas A, Vijayaraghavan GR, Kopans DB. Digital breast tomosynthesis: state of the art. *Radiology* 2015;**277**:663–84. https://doi.org/10.1148/radiol.2015141303.
8. Olgar T, Kahn T, Gosch D. Average glandular dose in digital mammography and breast tomosynthesis. *Röfo* 2012;**184**:911–8. https://doi.org/10.1055/s-0032-1312877.
9. Igarashi T. Radiation exposures in mammography and breast tomosynthesis. *NICHIDOKU-HO* 2016;**61**:68–77.
10. European Reference Organization for Quality Assured Breast Screening and Diagnostic Services. *Protocol for the quality control of the physical and technical aspects of digital breast tomosynthesis systems version 1.01*. 2016. Netherlands.
11. Dance DR, Young KC, van Engen RE. Further factors for the estimation of mean glandular dose using the United Kingdom, European and IAEA breast dosimetry protocols. *Phys Med Biol* 2009;**54**:4361–72. https://doi.org/10.1088/0031-9155/54/14/002.
12. Dance DR, Young KC, van Engen RE. Estimation of mean glandular dose for breast tomosynthesis: factors for use with the UK, European and IAEA breast dosimetry protocols. *Phys Med Biol* 2011;**56**:453–71. https://doi.org/10.1088/0031-9155/56/2/011.
13. Dance DR. *Breast dosimetry in digital mammography and tomosynthesis*. United Kingdom: NCCPM, Royal Surrey County Hospital; 2009. http://win.gisma.it/atti/peschiera09/corso_fisici_tsrm/dance_dosimetry_tomosynthesis_gisma_2009.pdf [accessed 08.05.18].
14. Bouwman RW, van Engen RE, Young KC, den Heeten GJ, Broeders MJ, Schopphoven S, et al. Average glandular dose in digital mammography and digital breast tomosynthesis: comparison of phantom and patient data. *Phys Med Biol* 2015;**60**:7893–907. https://doi.org/10.1088/0031-9155/60/20/7893.
15. ICRP pregnancy and medical radiation. Publication 84. *Ann ICRP* 2000;**30**(1).
16. Japan Network for Research and Information on Medical Exposure. *Diagnostic reference levels based on latest surveys in Japan —Japan DRLs 2015—*. 2015. http://www.radher.jp/J-RIME/report/DRLhoukokusyoEng.pdf [accessed 07.05.18].